© 2020. Published by The Company of Biologists Ltd | Journal of Cell Science (2020) 133, jcs244020. doi:10.1242/jcs.244020

RESEARCH ARTICLE

The lncRNA *MEG3* mediates renal cell cancer progression by regulating *ST3Gal1* transcription and EGFR sialylation

Aihong Gong[1,2,*], Xinyu Zhao[1,*], Yue Pan[1], Yu Qi[1], Shuangda Li[1], Yiran Huang[1], Yanru Guo[1], Xia Qi[1], Wei Zheng[3,‡] and Li Jia[1,‡]

ABSTRACT

Long noncoding RNAs (lncRNAs) have emerged as important regulators of cancer progression. Abnormal sialylation leads to renal cell carcinoma (RCC) malignancy. However, the mechanism by which the lncRNA maternally expressed gene 3 (*MEG3*) mediates RCC progression by regulating *ST3Gal1* transcription and EGFR sialylation is still unrevealed. Here, we found that the expression of *MEG3* was higher in adjacent tissues than in RCC tissues, as well as downregulated in RCC cell lines compared to expression in normal renal cells. The proliferation, migration and invasion of RCC cells transfected with *MEG3* was decreased, whereas knockdown of *MEG3* had the opposite effect. The proliferative and metastatic abilities of RCC cells *in vivo* were concordant with their behavior *in vitro*. *ST3Gal1* expression was dysregulated in RCC and was positively correlated with *MEG3*. By applying bioinformatics, c-Jun (also known as JUN) was identified as a transcription factor predicted to bind the promoter of *ST3Gal1*, and altered *MEG3* levels resulted in changes to c-Jun expression. Furthermore, ST3Gal1 modulated EGFR sialylation to inhibit EGFR phosphorylation, which affected activation of the phosphoinositide 3-kinase (PI3K)–AKT pathway. Taken together, our findings provide a novel mechanism to elucidate the role of the *MEG3*–ST3Gal1–EGFR axis in RCC progression.

KEY WORDS: Renal cell carcinoma, MEG3, ST3Gal1, EGFR

INTRODUCTION

Renal cell carcinoma (RCC), arising from the epithelium of renal tubules, is a common cancer worldwide (Lopez-Beltran et al., 2006). Once metastasis occurs in RCC, the median survival of patients is ∼8 months (Chen and Kuo, 2016); half of patients who present with metastasis die within the first year and only 10% of such patients survive longer than five years (Motzer et al., 2004; Rini, 2006). Radiation therapy and surgical excision remain the main method of therapy in RCC (Banumathy and Cairns, 2010; Lopez-Beltran et al., 2006). Thus, it is essential to identify novel diagnostic markers and effective therapeutic targets for RCC patients.

Long noncoding RNAs (lncRNAs), a type of non-protein-coding RNA, are reported to participate in diverse biological processes, including transcriptional regulation, cell differentiation, cell apoptosis, cancer cell metastasis, chemotherapy drug resistance, and RNA alternative splicing (Dinger et al., 2008; Ponting et al., 2009; Seles et al., 2016). Several lncRNAs have been well characterized in RCC, such as *HOTAIR* (Chiyomaru et al., 2014). *MALAT* (Hirata et al., 2015), *H19* (Raveh et al., 2015), and maternally expressed gene (*MEG3*) (Wang et al., 2015b). *HOTAIR* knockdown reduces the proliferation, migration and tumorigenicity of RCC (Wu et al., 2014). *MALAT1* expression is higher in RCC tissue compared to normal tissue, which enhances RCC cell progression and can be a prognostic clinical parameter (Ji et al., 2003). Knockdown of *H19* results in decreased growth, migration, and invasion of RCC. Higher expression of *H19* is associated with significantly shorter overall survival of RCC patients (Wang et al., 2015a). For *MEG3*, however, it has been only reported that the apoptotic rate is increased in RCC cell lines after transfection with this lncRNA (Wang et al., 2015b), and the biological function and regulatory mechanism of *MEG3*'s involvement in RCC progression are unknown.

Sialic acids are widely distributed in nature as terminal sugars of oligosaccharide chains of glycoconjugates (glycoproteins and glycolipids), which are important posttranslational modifications during cancer progression (Harduin-Lepers et al., 1995; Warren et al., 1972). Sialyltransferases (STs) are key enzymes in the biosynthesis of sialic acid, which contains oligosaccharides and glycoconjugates (Pilatte et al., 1993). It has been reported that β-galactoside α-2,3-sialyltransferase 1 (ST3Gal1) is an independent adverse prognostic factor for recurrence in RCC patients who underwent nephrectomy (Bai et al., 2015). However, relevant studies of untreated RCC patients is rare. The transcription factor c-Jun (also known as JUN) has been reported to play an important role in regulating cancer progression. However, there is no idea about the relationship between c-Jun and ST3Gal1.

Epidermal growth factor receptor (EGFR), which possesses tyrosine kinase activity, is a 170 kDa transmembrane glycoprotein with an extracellular ligand-binding domain and an intracellular region (Schlessinger, 2014; Wee and Wang, 2017). EGFR can activate several signaling pathways and highly correlates with cell proliferation, differentiation, drug sensitivity, and angiogenesis (Veale et al., 1993). Furthermore, the overexpression of EGFR is associated with shorter survival in non-small cell lung cancer (Mendelsohn and Baselga, 2006). EGFR is also phosphorylated in RCC, and stimulates the activation of phosphoinositide 3-kinase (PI3K), which leads to AKT translocation and localization. The EGFR–PI3K–AKT pathway is frequently overexpressed in RCC (Cancer Genome Atlas Research Network et al., 2016; Stumm et al., 1996). EGFR sialylation suppresses its phosphorylation in lung

[1]College of Laboratory Medicine, Dalian Medical University, Dalian 116044, Liaoning Province, China. [2]Department of Clinical Laboratory, Dermatology Hospital of Dalian, Dalian 116000, Liaoning Province, China. [3]Department of Urology, the First Affiliated Hospital of Dalian Medical University, Dalian 116011, Liaoning Province, China.
*These authors contributed equally to this work

‡Authors for correspondence (linjian0198@sina.com; zhengweimiwei@163.com)

A.G., 0000-0001-9737-7960; X.Z., 0000-0002-3385-7970; Y.P., 0000-0001-9538-0162; Y.Q., 0000-0002-6844-7373; S.L., 0000-0002-3286-444X; Y.H., 0000-0002-6932-0382; Y.G., 0000-0002-0464-8360; X.Q., 0000-0002-6361-7230; W.Z., 0000-0001-8518-9540; L.J., 0000-0003-2400-1991

Handling Editor: Daniel Billadeau
Received 17 January 2020; Accepted 20 July 2020

Journal of Cell Science (2020) 133, jcs244020. doi:10.1242/jcs.244020

cancer cells (Liu et al., 2011). However, the molecular mechanism of EGFR sialylation in RCC progression requires further investigation.

In this study, the expression of *MEG3* was assessed in RCC tissues and cell lines. Alterations in *MEG3* expression were associated with the proliferative and invasive abilities of RCC cells. Furthermore, the underlying mechanism involved in *MEG3*–ST3Gal1–EGFR-mediated EGFR sialylation and PI3K–AKT activation in RCC was explored.

RESULTS

The lncRNA *MEG3* is downregulated in RCC tissues and cell lines

To determine the expression pattern of *MEG3* in RCC tissues and cell lines, reverse-transcription qPCR (RT-qPCR) was performed. As shown in Fig. 1A, *MEG3* expression was downregulated in RCC tissues (2.99±1.45, mean±s.d.) compared with related adjacent normal tissues (5.06±1.67, mean±s.d.). Fluorescence *in situ* hybridization (FISH) was also performed in RCC tissues and adjacent tissues to identify the location of *MEG3* expression. According to the fluorescence signal, RCC tissues exhibited lower fluorescence intensity of *MEG3* than adjacent tissues, and *MEG3* showed high expression in cell nuclei (Fig. 1B). As shown in Fig. 1C, 293T cells exhibited high levels of *MEG3*, while RCC cell lines 786-O, ACHN and Caki-1 presented lower *MEG3* relative expression levels (0.70±0.05, 0.49±0.138, and 0.39±0.11, respectively; mean±s.d.). These results indicated that a low level of *MEG3* might be associated with RCC.

The lncRNA *MEG3* mediates RCC cell growth and migration *in vitro*

Given the downregulated expression of *MEG3* in RCC tissues and cell lines, we performed loss-of-function and gain-of-function studies in 786-O cells. A CCK-8 cell-counting assay was performed after cells were transfected with *MEG3* or siRNA targeting *MEG3* (si*MEG3*). The results indicated that *MEG3* overexpression impaired cell proliferation, whereas knockdown of *MEG3* promoted cell proliferation *in vitro* (Fig. 2A,B). As shown in Fig. 2C and D, the migratory ability was decreased after cells were transfected with *MEG3*, while the ability was recovered in *MEG3* knockdown cells, as determined by wound healing assays. The effect of *MEG3* on RCC cell invasion was reversed when cells were transfected with si*MEG3*, as determined using Transwell assays (Fig. 2E,F). In addition, ACHN cells showed the same trend (Fig. S1). All data indicated that *MEG3* might play an important role in RCC progression.

The lncRNA *MEG3* mediates RCC cell growth and metastasis *in vivo*

We performed tumorigenicity assays and tail-vein injection assays in nude mice. To confirm whether *MEG3* affected RCC tumorigenesis, 786-O cells were transfected with vector, *MEG3*, control scrambled shRNA (shSCR), or an shRNA targeting *MEG3* (sh*MEG3*), and injected into the right flank of nude mice. After 28 d, the mice were killed and xenograft tumors were taken for further research. Tumor volume was smaller in the mice treated with *MEG3* than in those treated with the vector control, whereas the sh*MEG3* group showed opposite result (Fig. 3A). Ki67 levels were measured by immunohistochemistry (IHC) staining (Fig. 3B,C). To further verify that *MEG3* affected cell metastasis, 786-O cells transfected with *MEG3* or sh*MEG3* were injected into tail veins of nude mice. As expected, the *MEG3* group showed lower near-infrared fluorescence intensity than the vector group, whereas *MEG3* knockdown resulted in increased fluorescence intensity (Fig. 3D). The nude mice bearing 786-O cells transfected with *MEG3* showed attenuated lung metastasis, whereas knockdown of *MEG3* facilitated lung metastasis of 786-O cells (Fig. 3E). These data indicated promising therapeutic targets for RCC malignancy.

The lncRNA *MEG3* regulates *ST3Gal1* transcription via interaction with the transcription factor c-Jun

Aberrant sialylation is closely associated with the malignant phenotype of cancer cells, including metastatic potential and invasiveness (Miyagi, 2008). To further research the relationship between STs and RCC, the expression of ST3Gal1 was detected in RCC. We found that ST3Gal1 mRNA and protein expression was lower in RCC tissues than in adjacent tissues by IHC staining (Fig. 4A) and RT-qPCR (Fig. 4B). A significant positive correlation was observed between *MEG3* and ST3Gal1 ($r=0.4736$, $P<0.0001$; Fig. S2). In addition, the mRNA and protein levels of ST3Gal1 were detected after cells were transfected with *MEG3* or si*MEG3*. The aberrant expression of *MEG3* regulated ST3Gal1 mRNA and protein levels (Fig. 4C,D). According to FISH, *MEG3* was mostly located in nuclei (Fig. 4E). Moreover, overexpression of *MEG3*

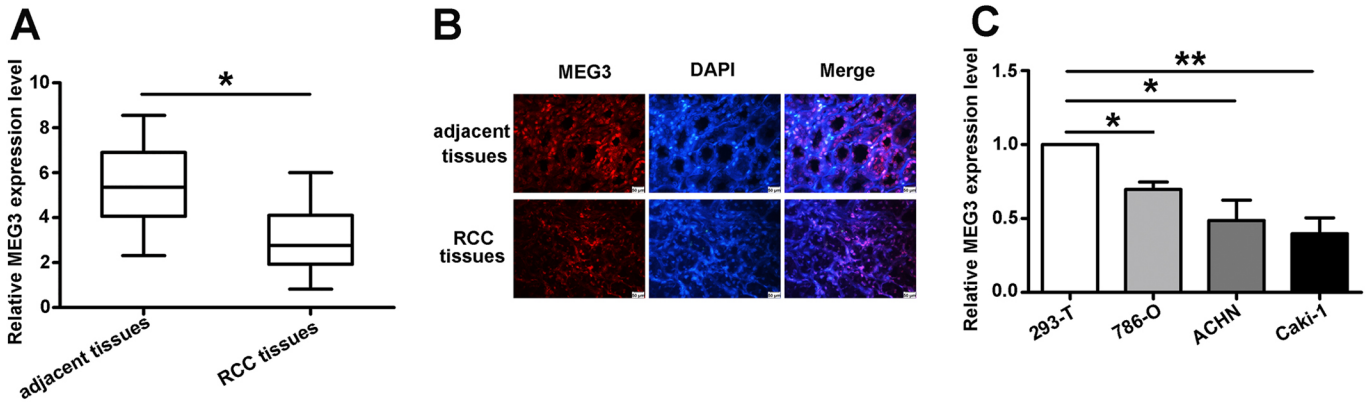

Fig. 1. The lncRNA *MEG3* is downregulated in RCC tissues and cell lines. (A) Relative *MEG3* expression in RCC tissues and adjacent tissues, as detected by RT-qPCR. Box and whisker plot shows the median (line), interquartile range (box) and range (whiskers). (B) A FISH staining assay was performed in RCC tissues and adjacent tissues. (C) Relative MEG3 expression was tested in RCC cell lines and human embryonic kidney 293-T (HEK293-T) cells. Data in A and C are mean±s.d. Each experiment was repeated three times. *$P<0.05$; **$P<0.01$ (unpaired two-tailed *t*-test). Scale bars: 50 µm.

Journal of Cell Science (2020) 133, jcs244020. doi:10.1242/jcs.244020

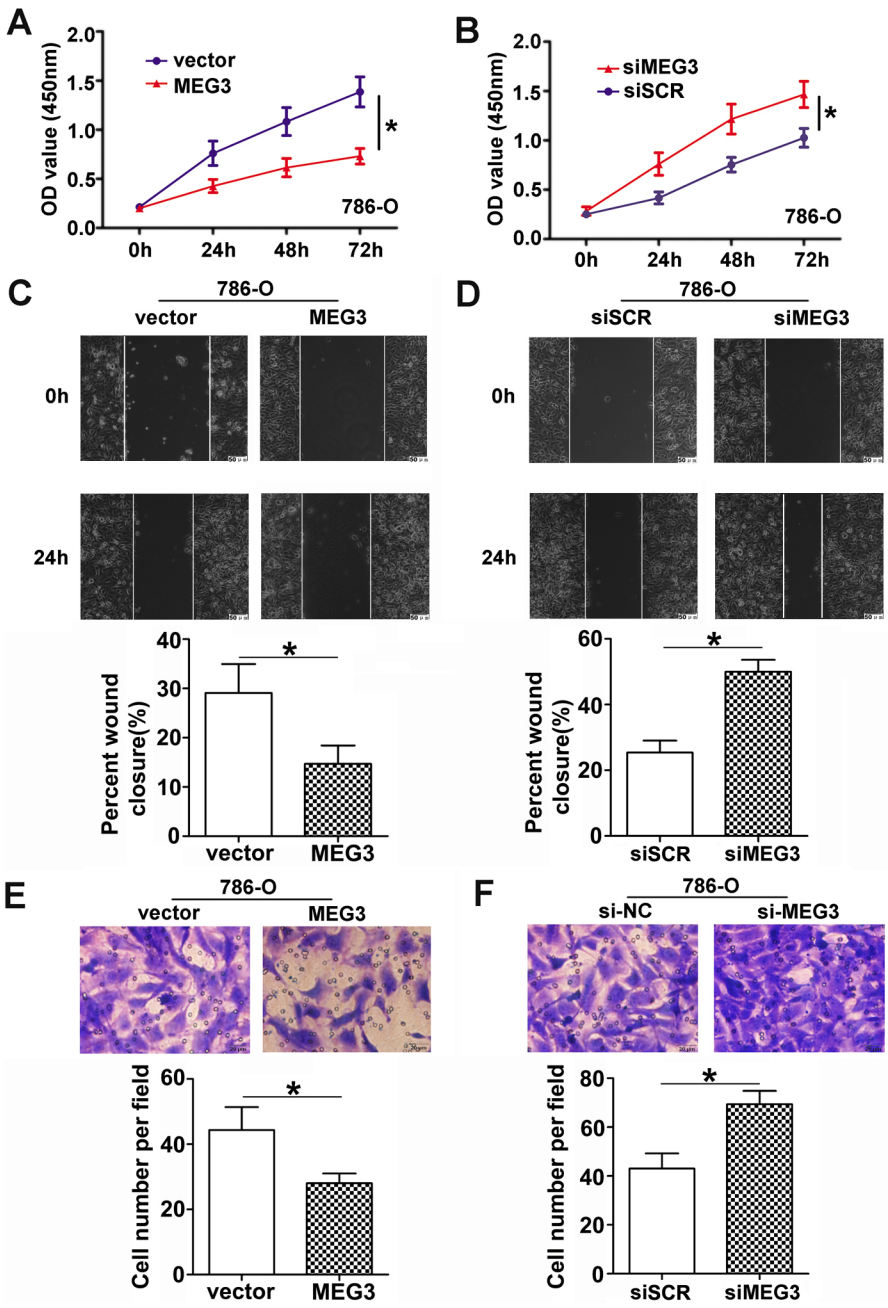

Fig. 2. The lncRNA *MEG3* mediates 786-O cell growth and metastasis *in vitro*. (A,B) A CCK-8 assay was performed to evaluate the proliferative ability of 786-O cells after transfection with *MEG3* or si*MEG3*. (C,D) A wound healing assay was used to investigate the effects of *MEG3* overexpression (C) or knockdown (D; siSCR indicates control non-targeting siRNA) on the migratory ability of 786-O cells. Representative images taken at 0 h and 24 h are shown. White lines indicate the edge of the wound. Scale bars: 50 µm. (E,F) The effect of *MEG3* overexpression (E) or knockdown (F) on 786-O cell invasion was determined using Transwell assays. Scale bars: 20 µm. Data are mean±s.d. of three experiments. **P*<0.05 (unpaired two-tailed *t*-test).

obviously elevated transcriptional activity of the *ST3Gal1* promoter, as determined using a luciferase reporter assay (Fig. 4F).

To investigate the potential regulators involved in ST3Gal1 expression, bioinformatics software was used to scan for potential transcription-factor-binding sites in the *ST3Gal1* promoter. According to the bioinformatics predictions, c-Jun was identified as a candidate transcription factor that regulates the *ST3Gal1* promoter through direct binding (Fig. 4G). Knockdown of c-Jun promoted ST3Gal1 mRNA and protein levels (Fig. 4H). A chromatin immunoprecipitation (ChIP) assay was performed to prove that c-Jun directly bound to the *ST3Gal1* promoter (Fig. 4I).

It has been reported that c-Jun transactivation activity is inhibited by its interaction with *MEG3* (Zhou et al., 2017). To verify this conclusion, an RNA immunoprecipitation assay (RIP) and western blot analysis were performed to figure out the relationship between *MEG3* and c-Jun in RCC cells. As shown in Fig. 4J, altered *MEG3* levels regulated the expression of c-Jun. The RIP assay further evaluated the specific interaction between *MEG3* and c-Jun. The results suggested that *MEG3* positively regulated *ST3Gal1* mRNA transcription by interacting with c-Jun (Fig. 4K).

MEG3 and ST3Gal1 modulate EGFR phosphorylation and PI3K–AKT activation in RCC cells

It has been reported that EGFR sialylation suppresses EGFR phosphorylation by inhibiting EGF binding and EGFR dimerization (Yen et al., 2015). To verify this conclusion, phosphorylation of EGFR was detected following treatment with EGF in 786-O cells transfected with ST3Gal1 or siRNA targeting ST3Gal1 (siST3Gal1). According to Fig. 5A, EGFR phosphorylation was reduced in 786-O cells transfected with ST3Gal1. In contrast, the level of EGFR phosphorylation was increased in siST3Gal1 cells (Fig. 5B). In the presence of EGF, the EGFR phosphorylation level was inhibited after

Journal of Cell Science (2020) 133, jcs244020. doi:10.1242/jcs.244020

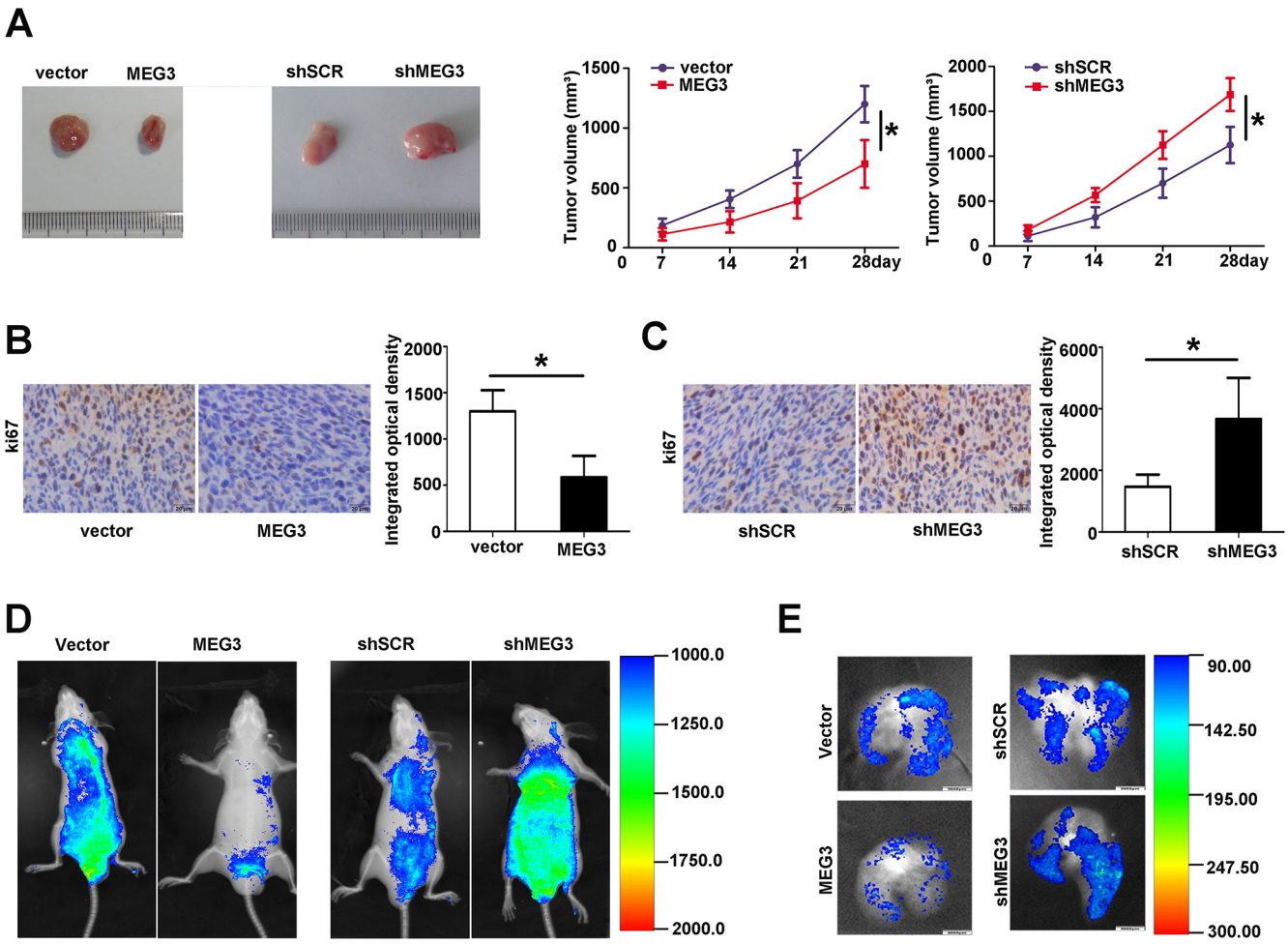

Fig. 3. The lncRNA *MEG3* mediates RCC cell growth and metastasis *in vivo*. (A) 786-O cells stably overexpressing *MEG3* (MEG3) or with knockdown of *MEG3* (sh*MEG3*), alongside vector only and scrambled shRNA (shSCR) controls, respectively, were injected into flanks of nude mice. The volumes of xenograft tumors were calculated and analyzed. Scale bar graduations are 1 mm. (B,C) Ki-67 was examined by IHC staining in xenograft tumors to evaluate the effect of *MEG3* on the proliferation of 786-O cells. Scale bars: 20 µm. (D,E) A metastatic animal model was assayed by injecting 786-O cells transfected with *MEG3* or sh*MEG3* into the tail vein of nude mice. Each mouse was subjected to fluorescence (near infra-red, NIR) and X-ray imaging using a Kodak Imaging Station imaging system, and the two images were superimposed for tumor localization (D). The lung metastasis degree of transfected 786-O cells was assessed (E). Representative images of a total of 24 animals are shown. Scale bar: 5000 µm. Color scale indicates the degree of lung metastasis. Data in A–C are mean±s.d. Each experiment was repeated three times. **P*<0.05 (unpaired two-tailed *t*-test).

ST3Gal1 overexpression, whereas the effect was reversed when 786-O cells transfected with siST3Gal1 were treated with EGF (Fig. 5A,B).

Considering that c-Jun regulated ST3Gal1, which was mediated by *MEG3*, we supposed that a *MEG3*–c-Jun–ST3Gal1 axis might regulate phosphorylated EGFR. To confirm this supposition, EGFR was measured after transfecting cells with *MEG3* or si*MEG3* upon EGF stimulation. As shown in Fig. 5C, overexpression of *MEG3* increased EGFR affinity for the lectin MAL by elevating *ST3Gal1* levels in 786-O cells compared to the control groups, as measured by lectin affinity assay. Conversely, treatment of 786-O cells with si*MEG3* reduced EGFR affinity for the lectin MAL, by inhibiting *ST3Gal1* expression.

Seeing that disruption of EGFR activity can regulate downstream signaling, including the AKT–PI3K–mTOR pathway (Bai et al., 2015), we examined the effect of *MEG3* on this EGFR-mediated intracellular signaling pathway in 786-O cells. The protein levels of phosphorylated EGFR, PI3K p110α (encoded by *PIK3CA*) and phosphorylated AKT were reduced upon EGF stimulation in 786-O cells transfected with *MEG3* compared with levels in control cells (Fig. 5D). The total level of EGFR and AKT proteins remained unchanged. Upon EGF stimulation, 786-O cells treated with si*MEG3* showed stronger phosphorylation of PI3K–Akt pathway components compared to levels in control cells (Fig. 5D). Furthermore, the same trend was observed in ACHN cells (Fig. S3). The data suggested that *MEG3* influences EGFR phosphorylation and leads to the activation of the PI3K–AKT pathway in RCC cells by modulating ST3Gal1 levels.

DISCUSSION

The lncRNA *MEG3*, as a tumor suppressor, has been confirmed to take part in cancer progression. *MEG3* was found to inhibit the proliferation of RCC cells by inducing G2/M cell-cycle arrest and apoptosis (Qin et al., 2013). *MEG3* is downregulated in most RCC tissues and lowly expressed in RCC cell lines 786-O and SN12. The viability of 786-O cells is reduced, and the apoptosis rate is enhanced after overexpression of *MEG3* (Qin et al., 2013). In this study, differential expression of *MEG3* was shown in RCC samples and RCC cell lines. Moreover, *MEG3* mediated the proliferation, migration, invasion and metastasis of RCC cells both *in vitro* and *in vivo*. Therefore, *MEG3* is implicated as a tumor suppressor in RCC progression.

Journal of Cell Science (2020) 133, jcs244020. doi:10.1242/jcs.244020

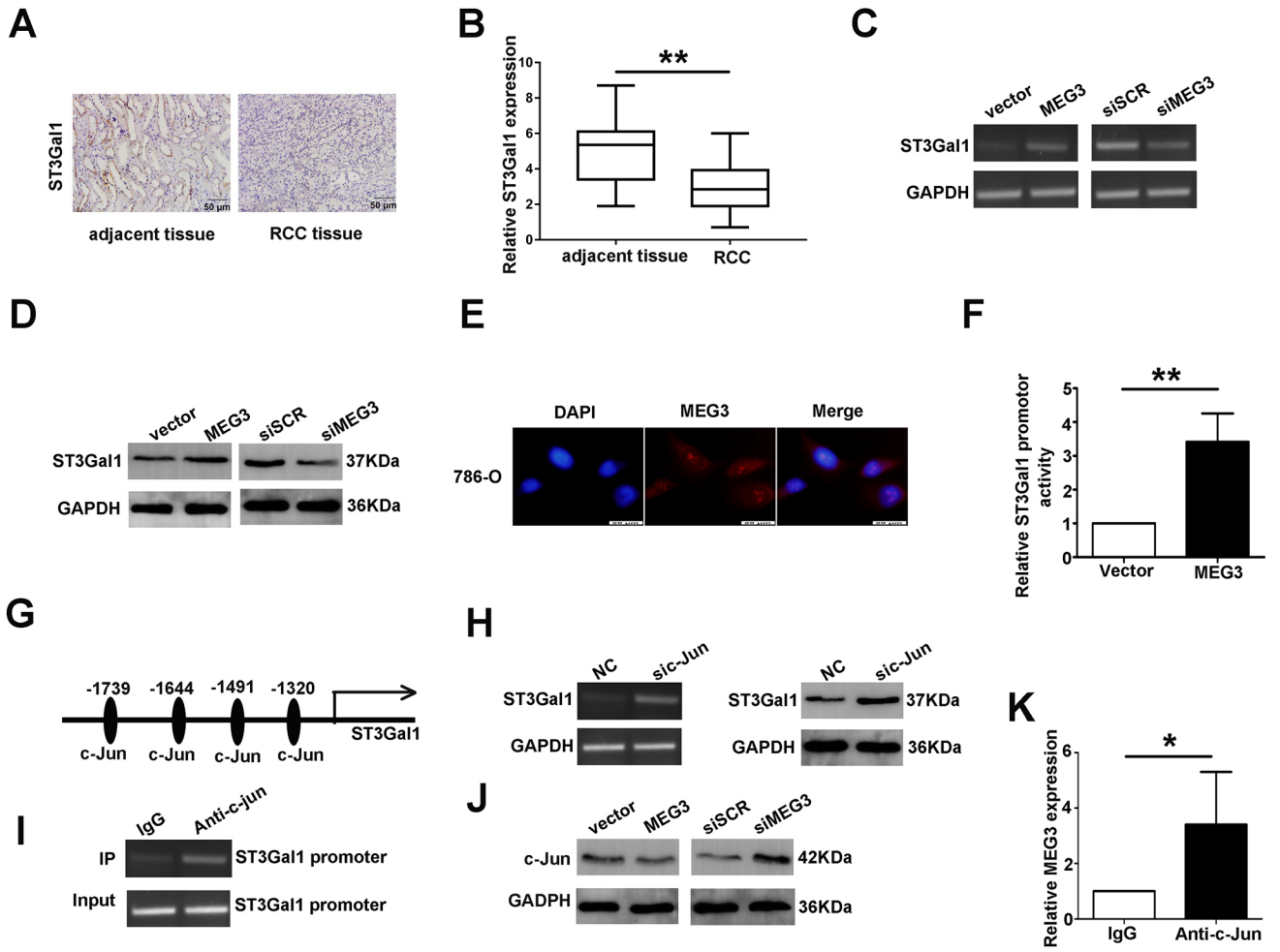

Fig. 4. The lncRNA *MEG3* regulates *ST3Gal1* transcription via interaction with the transcription factor c-Jun. (A) ST3Gal1 expression was analyzed in RCC tissue and adjacent tissue using IHC staining. Scale bars: 50 µm. (B) Relative *ST3Gal1* level was detected in RCC tissues and adjacent tissues by RT-qPCR. (C,D) Total RNA and protein was extracted from 786-O cells transfected with *MEG3* or si*MEG3*, alongside control cells transfected with an empty vector or scrambled siRNA (siSCR). The mRNA level of *ST3Gal1* was analyzed by RT-PCR (C), and the protein level of ST3Gal1 was assayed by western blotting (D). GAPDH was used a loading control. (E) FISH assay performed on 786-O cells to determine the location of *MEG3*. Scale bars: 20 µm. (F) *ST3Gal1* promoter-driven luciferase reporter constructs were co-transfected with *MEG3* into 786-O cells. Promoter activity is shown relative to the vector only control. (G) Potential transcription factor binding sites in the *ST3Gal1* promoter region (−2000 bp to +0 bp) were analyzed. Positions (in bp) of predicted c-Jun binding sites relative to the transcription start site are indicated. (H) The mRNA and protein levels of ST3Gal1 were measured in 786-O cells transfected with si-c-Jun by RT-PCR and western blot, and compared to levels in cells transfected with a control siRNA (NC). (I) ChIP assays were performed to determine c-Jun binding to the *ST3Gal1* promoter. (J) The protein level of c-Jun was detected in 786-O cells transfected with *MEG3* or si*MEG3* by western blotting. (K) An RNA Immunoprecipitation (RIP) assay was used to evaluate the specific interaction of *MEG3* with c-Jun. Box and whisker plot in B shows the median (line), interquartile range (box) and range (whiskers). Data in F and K are mean±s.d. Each experiment was repeated three times. **P*<0.05, ***P*<0.01 (unpaired two-tailed *t*-test).

Sialylation, a common glycosylation posttranslational modification, plays roles in regulating cellular interactions and signal transduction. ST3Gal1 mediates the transfer of sialic acid with an α2,3-linkage to terminal galactose residues. High expression of ST3Gal1 is associated with advanced stage epithelial ovarian cancer (Wen et al., 2017). Altered levels of ST3GAL1 correspond to the drug-resistant phenotype of chronic myeloid leukemia (CML) cell lines (Li et al., 2016). However, similar studies of the role of ST3Gal1 in RCC are rare. According to The Cancer Genome Atlas (https://portal.gdc.cancer.gov/) and our research, we found that ST3Gal1 showed higher expression in adjacent tissues than in RCC tissues. The ST3Gal1 level was regulated by *MEG3*, and a positive correlation between *MEG3* and ST3Gal1 expression was shown.

The c-Jun transcription factor has been reported as a positive regulator of cell proliferation. The growth-promoting activity of c-Jun is regulated by repression of tumor suppressors, such as tumor-suppressor PTEN (Shaulian and Karin, 2002). Other studies also demonstrated that c-Jun is a negative transcription factor, which negatively regulates *PHLPP1* transcription by binding directly to the *PHLPP1* promoter (Zhou et al., 2017). Here, *MEG3* mediated c-Jun activity, which negatively regulated *ST3Gal1* transcription by binding directly to the *ST3Gal1* promoter. We reported that the lncRNA *MEG3* participated in the protein sialylation process by regulating *ST3Gal1* at the transcriptional level.

EGFR is commonly upregulated in cancers such as metastatic colorectal cancer, glioblastoma, pancreatic cancer, and breast cancer (Li et al., 2016; Shaulian and Karin, 2002; Wen et al., 2017). EGF binds to the exposed dimerization interface of EGFR for receptor activation. After autophosphorylation, dimeric EGFR recruits and activates various downstream signaling proteins. It has been reported that EGFR phosphorylation is suppressed after EGFR sialylation (Shaulian and Karin, 2002). However, EGFR phosphorylation has garnered considerably less research attention in RCC. In this study, the level of phosphorylated EGFR was assayed in ST3Gal1-regulated

Journal of Cell Science (2020) 133, jcs244020. doi:10.1242/jcs.244020

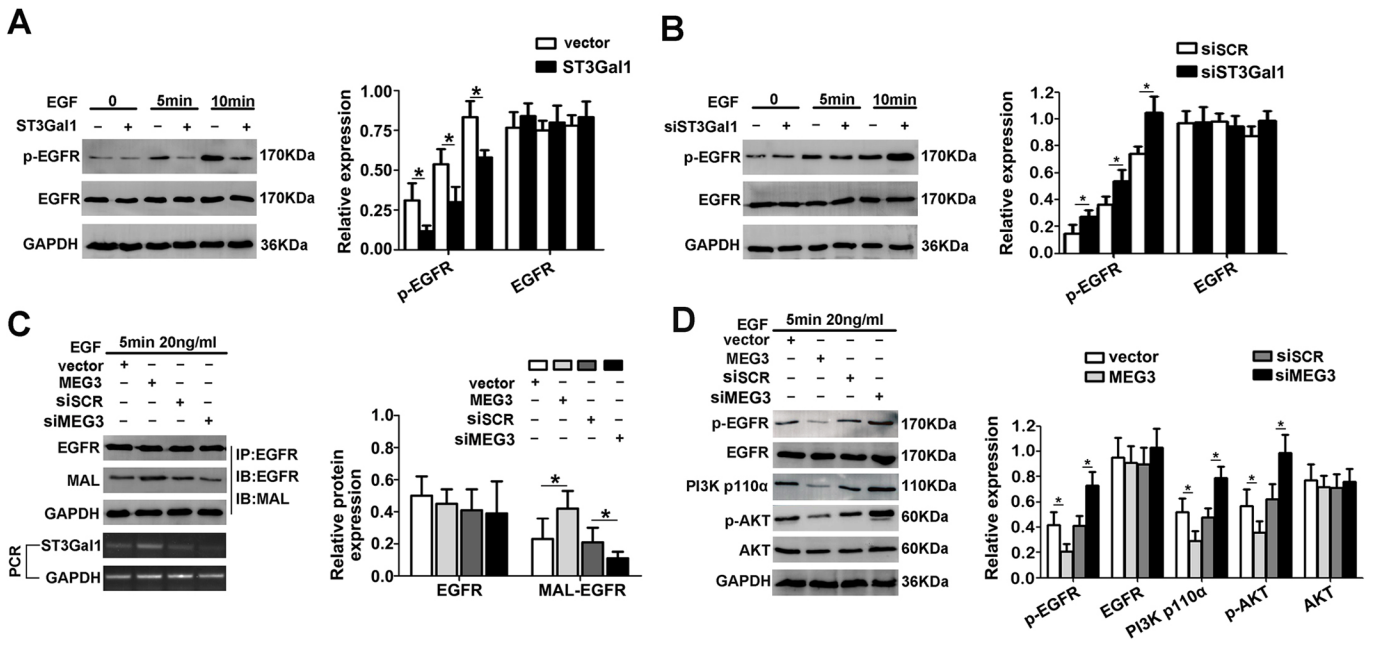

Fig. 5. *MEG3* and ST3Gal1 modulate EGFR phosphorylation in 786-O cells. (A,B) The phosphorylation of EGFR and total EGFR were detected in 786-O cells transfected with ST3Gal1 (ST3Gal1 +) or siST3Gal1 (ST3Gal1 –) upon EGF (20 ng/ml) stimulation for 0, 5, and 10 min using western blotting. (C) 786-O cells were transfected with *MEG3* or si*MEG3*, alongside the respective vector only and scrambled siRNA (si-SCR) controls. EGFR expression upon EGF (20 ng/ml) stimulation for 5 min was evaluated by western blot. Sialylation of EGFR was analyzed using a MAL lectin affinity assay. RT-PCR was used to detect *ST3Gal1* expression. (D) Alteration of *MEG3* impacted the activity of PI3K–AKT signaling in 786-O cells transfected with *MEG3* or si*MEG3* in the presence of EGF (20 ng/ml, for 5 min), as assayed by western blotting. GAPDH is shown as a loading control. Data are mean±s.d. Each experiment was repeated three times. **P*<0.05 (unpaired two-tailed *t*-test).

cells. The results consistently showed that downregulation of ST3Gal1 promoted EGFR phosphorylation. Additionally, phosphorylated EGFR expression was regulated through sialylation by ST3Gal1, mediated by *MEG3*. According to the outcome, sialylation of EGFR might be potential marker for RCC diagnosis.

EGFR signaling is a complicated network regulated by its phosphorylation. Upon activation of EGFR, various adaptor and effector molecules are activated, triggering several signaling cascades, such as the PI3K–AKT pathway. Furthermore, phosphorylated (Y920) EGFR can dock with PI3K, which inactivates the apoptotic cascade via BAD (Bcl2-associated death factor) and caspase-9 (Datta et al., 1997). Here, we focused on the effect of the *MEG3*–c-Jun–ST3Gal1 axis on phosphorylated EGFR and the signaling molecules AKT and PI3K in RCC cell lines. Alteration of *MEG3* mediated the activation of EGFR, as well as inducing PI3K–AKT pathway activation. It is reasonable to conclude that the promotional effects of *MEG3* on RCC progression could at least be partially mediated via elevated EGFR-mediated PI3K–AKT signaling.

In summary, our study defines a mechanism in which *MEG3* acts as a tumor suppressor that regulates ST3Gal1 by interacting with c-Jun. Sialylation of EGFR inhibits EGFR phosphorylation and PI3K–AKT pathway activation. However, the mechanisms of RCC progression are multiple and complicated, and further investigations should be made to explore the *MEG3*–c-Jun–ST3Gal1–EGFR crosstalk in RCC progression.

MATERIALS AND METHODS

Cell culture

Human RCC cell lines 786-O, Caki-1, ACHN were purchased from KeyGEN Company (Nanjing, China). ACHN and 293T cells were cultured in Modified Eagle's medium (MEM) supplemented with 10% fetal bovine serum (FBS, Gibco, Grand Island, NY). 786-O and Caki-1 were maintained in RPMI-1640 supplemented with 10% FBS in a humidified atmosphere of 5% CO_2, maintained at 37°C. *MEG3* was cloned into the pcDNA3.1 vector (Invitrogen) for expression. si*MEG3*, si*SCR*, sh*MEG3* and shSCR were synthesized by GenePharma. Lipofectamine 3000 reagents (Invitrogen Co., Carlsbad, CA, USA) were used for cell transfection.

Patient tissue samples

Thirty pairs of RCC tissues and adjacent non-tumor tissues were collected from patients who underwent surgical resections at the First Affiliated Hospital of Dalian Medical University from January 2016 to September 2018, after obtaining informed consent. The investigation project and the informed consent have been approved by the Ethics Committee of the First Affiliated Hospital of Dalian Medical University (Ethics Reference No: YJ-KY-FB-2016-37) and all investigations were conducted according to the principles expressed in the Declaration of Helsinki. The specimens were frozen in liquid nitrogen and stored at −80°C.

RNA isolation and quantitative real-time PCR analysis

TRIZOL reagent (Invitrogen, Carlsbad, CA, USA) was used to isolate total RNA. RT-qPCR analysis was performed using SYBR-Green quantitative RT-PCR Master Mix kit (TIANGEN BIOTECH, Beijing, China). The sequences of the upstream and downstream primers were as follows: 5′-GCCAGCTGTCCCTCTTACCTAA-3′ (F) and 5′-TCCAGTTTGCTAGCAGGTGAAC-3′ (R) for *MEG3*, 5′-ATGGTGACCCTGCGGAAGA-3′ (F) and 5′-TCATCTCCCCTTGAAGATCC-3′ (R) for *ST3Gal1*, and 5′-ACCACAGTCCATGCCATCAC-3′ (F) and 5′-TCCACCACCCTGTTGCTGTA-3′ (R) for *GAPDH*. The $2^{-\Delta\Delta Ct}$ method was used for quantification, and fold change for target genes was normalized using an internal control. Each experiment was repeated three times.

EGF stimulation and cell extraction

The activation of EGFR was tested in serum-deprived cells by adding 20 ng/ml EGF for 5 or 10 min. Ice-cold 10% trichloroacetic acid was used to stop the reaction. The cellular precipitates were scraped and collected by

centrifugation at 14,000 ***g*** for 5 min. Cells were washed with PBS, scraped and solubilized on ice for 15 min in RIPA buffer (50 mM Tris-HCl pH 7.4, 150 mM NaCl, 1% Triton X-100, 1% sodium deoxycholate and 0.1% SDS) and protease inhibitor cocktail (200 mM AEBSF, 30 µM Aprotinin, 13 mM Bestatin, 1.4 mM E64 and 1 mM Leupeptin). The protein concentration of the cell extract was tested using a BCA kit.

Western blotting and lectin affinity assay

Cell extracts were electrophoresed by SDS–PAGE. Proteins were transferred to a PVDF membrane. Non-specific binding was blocked with 5% skimmed milk for 2 h at 37°C. The membrane was incubated with anti-EGFR (1:1000 dilution; Abcam), anti-phospho-EGFR (1:1000 dilution; Abcam), anti-ST3Gal1 (1:1000 dilution; Abcam), anti-PI3K, anti-phospho-AKT, anti-AKT (all 1:1000 dilution; Abcam) or *Maackia amurensis* lectin (MAL, 1:2000, Vector, California, USA, Catalog. B-1315) at 4°C overnight. GAPDH antibody (1:1000 dilution; Abcam) was used as a control. α2,3-Sialylated EGFR was detected using a lectin affinity assay by immunoprecipitating lysates with the anti-EGFR antibody. The membrane was incubated with peroxidase-conjugated anti-rabbit IgG (1:2000 dilution; Abcam). Images were obtained using a multifunctional gel imaging system (Image Quant LAS 500, General Electric, Fairfield, CT, USA).

Luciferase reporter assay

The *ST3Gal1* promoter region was synthesized and inserted into a pGL3-basic vector (Promega, Madison, WI, USA). 786-O cells were co-transfected with the *ST3Gal1* promoter-driven luciferase reporter together with pGL3-*MEG3* or pGL3- basic vector. A Dual-Luciferase Assay Kit (Promega, Madison, WI, USA) was used to assess luciferase activities.

Transwell assays

The invasion assays were performed using 24-well transwell chambers (8 µm; Corning, Shanghai, China), and the upper chambers were covered with 1 mg/ml Matrigel at first. Tumor cells were resuspended in serum-free RPMI-1640 medium and 1.0×10^4 cells were seeded into the upper chambers. 0.5 ml RPMI-1640 containing 10% FBS was added to the bottom chambers. After 24-h incubation, cells on the upper surface of the membrane were scrubbed off, and the migrated cells were fixed in 75% methanol, stained with 0.1% crystal violet for 25 min, and counted under a light microscope (40× objective, 10× eyepiece magnification).

In vivo proliferation and metastasis assays

Four-week-old nude mice were purchased from the Model Animal Research Institute of Nanjing University. 5×10^6 cells stably transfected with *MEG3*, sh*MEG3* or control vector were injected into the right flank of every nude mouse by subcutaneous injection. Tumor size was determined every 7 d. After 28 d, the nude mice were killed, and tumors were isolated and weighed. Tumor volume was calculated as the following formula: (length×width^2)/2.

The GFP-labeled 786-O cells with different treatments were cultured in RPMI-1640 medium, resuspended at a concentration of 1×10^7 cells/200 µl, and injected subcutaneously into each mouse tail vein. After 3 weeks, mice were killed and lungs were harvested for fluorescence analysis. All lungs were imaged within 20–30 min after euthanasia. The representative X-ray and fluorescence images were captured to reveal the degree of lung metastasis *in vivo*. The images were taken using the *in vivo* Imaging System of Dalian Medical University. All animal experiments were performed according to approved guidelines.

Cell viability

The cell viability was performed using a Cell Counting Kit-8 (CCK-8; KeyGEN, Nanjing, China). 5×10^3 cells were seeded into 96-well plates with 100 µl of RPMI-1640 medium containing 10% FBS. 10 µl CCK-8 solution was added to the plate after incubation. The absorbance was measured in a microplate reader at 450 nm (168-1000 Model 680, Bio-Rad). Each experiment was performed three times.

Wound healing assay

4×10^5 cells were seeded in a 12-well plate. The following day, when adherent cells were observed, the cell layer was scratched using a pipette tip. Next, images of cell morphology were captured at the initiation time and for 24 h under an Olympus microscope (40× objective, 10× eyepiece magnification). The migratory ability was quantified and normalized to relative gap distance. The results of the experiments were analyzed using IPP6.0 software (MEDIA CYBERNETICS, USA).

Chromatin immunoprecipitation

Chromatin immunoprecipitation (ChIP) assays were performed using a ChIP chromatin immunoprecipitation kit (Beyotime, Shanghai, China). Immunoselections of cross-linked protein–DNA were performed using anti-c-Jun antibody (1:1000 dilution; Abcam) and proteinA/G agarose beads, at 4°C overnight. Anti-rabbit IgG was used as a negative control. Purified DNAs were analyzed by PCR.

RNA immunoprecipitation

The 786-O cells were lysed in RIP lysis buffer (N653-100 ml; Shanghai Hao Ran Biotechnology Co. Ltd., Shanghai, China). Then, the extract was incubated with magnetic beads conjugated with c-Jun antibody or control IgG for 6–8 h at 4°C. The beads were washed with washing buffer (EHJ-BVIS08102; Xiamen Huijia Biological Technology Co. Ltd., Xiamen, China) and incubated with proteinase K at 55°C for 30 min to remove the proteins. RNA was extracted using Trizol, and qPCR was performed to detect *MEG3* RNA present in the immune complex.

Fluorescence *in situ* hybridization

The RCC tissues, adjacent normal tissues and RCC cells were fixed in 10% formaldehyde, dehydrated in a dehydration series of alcohol and then embedded in paraffin. 0.5 mm thick slices were cut, dewaxed and rehydrated. The samples were digested with proteinase K for 15 min in 37°C, then denatured with formamide. The cells were incubated with Cy3-labeled *MEG3* probes at 73°C for 15 min and incubated at 37°C overnight. The slices were washed with 2×SSC for 3 min. DAPI (4′,6-diamidino-2-phenylindole) was used to counterstain the nuclei for 20 min in darkness. The samples were then scanned and photographed.

Immunohistochemistry

Immunohistochemistry (IHC) staining was performed on paraffin-embedded sections of tissue samples. Serial sections (5 µm each) were deparaffinized, rehydrated and immersed in 3% hydrogen peroxide for 10 min to block the endogenous peroxidase activity. The slices were incubated with the corresponding primary antibodies overnight at 4°C. After extensive washing with PBS, the secondary streptavidin–horseradish peroxidase-conjugated antibody staining was performed at room temperature, visualized using 3,3′-diaminobenzidine (DAB; ZLI9018, ZSGBBIO, China), then counterstained with Hematoxylin, dehydrated and cover-slipped.

Statistical procedures

Data are presented as the mean±s.d. Differences between two groups were assessed using an unpaired two-tailed *t*-test. $P<0.05$ was considered to be statistically significant. All results were reproduced across triplicate experiments. Statistical analyses were carried out using GraphPad Prism (GraphPad Software, Inc., USA).

Competing interests

The authors declare no competing or financial interests.

Author contributions

Conceptualization: L.J.; Methodology: Y.P.; Software: Y.P.; Validation: Y.Q.; Formal analysis: S.L., Y.G.; Investigation: A.G., Y.H.; Data curation: Y.Q., S.L., Y.H., Y.G.; Writing - review & editing: A.G., X.Z., X.Q., W.Z.; Supervision: L.J.; Project administration: L.J.; Funding acquisition: L.J.

Funding

This work was supported by a grant from the National Natural Science Foundation of China (81772277).

Supplementary information

Supplementary information available online at
https://jcs.biologists.org/lookup/doi/10.1242/jcs.244020.supplemental

Peer review history
The peer review history is available online at
https://jcs.biologists.org/lookup/doi/10.1242/jcs.244020.reviewer-comments.pdf

References

Bai, Q., Liu, L., Xia, Y., Long, Q., Wang, J., Xu, J. and Guo, J. (2015). Prognostic significance of ST3GAL-1 expression in patients with clear cell renal cell carcinoma. *BMC Cancer* **15**, 880. doi:10.1186/s12885-015-1906-5

Banumathy, G. and Cairns, P. (2010). Signaling pathways in renal cell carcinoma. *Cancer Biol. Ther.* **10**, 658-664. doi:10.4161/cbt.10.7.13247

Cancer Genome Atlas Research Network, Linehan, W. M. Spellman, P. T. Ricketts, C. J. Creighton, C. J. Fei, S. S. Davis, C. Wheeler, D. A. Murray, B. A. Schmidt, L. et al. (2016). Comprehensive molecular characterization of papillary renal-cell carcinoma. *N. Engl. J. Med.* **374**, 135-145. doi:10.1056/NEJMoa1505917

Chen, S. C. and Kuo, P. L. (2016). Bone metastasis from renal cell carcinoma. *Int. J. Mol. Sci.* **17**, 987. doi:10.3390/ijms17060987

Chiyomaruik, T., Fukuhara, S., Saini, S., Majid, S., Deng, G., Shahryari, V., Chang, I., Tanaka, Y., Enokida, H., Nakagawa, M. et al. (2014). Long non-coding RNA HOTAIR is targeted and regulated by miR-141 in human cancer cells. *J. Biol. Chem.* **289**, 12550-12565. doi:10.1074/jbc.M113.488593

Datta, S. R., Dudek, H., Tao, X., Masters, S., Fu, H., Gotoh, Y. and Greenberg, M. E. (1997). Akt phosphorylation of BAD couples survival signals to the cell-intrinsic death machinery. *Cell* **91**, 231-241. doi:10.1016/S0092-8674(00)80405-5

Dinger, M. E., Pang, K. C., Mercer, T. R. and Mattick, J. S. (2008). Differentiating protein-coding and noncoding RNA: challenges and ambiguities. *PLoS Comput. Biol.* **4**, e1000176. doi:10.1371/journal.pcbi.1000176

Harduin-Lepers, A., Recchi, M.-A. and Delannoy, P. (1995). 1994, the year of sialyltransferases. *Glycobiology* **5**, 741-758. doi:10.1093/glycob/5.8.741

Hirata, H., Hinoda, Y., Shahryari, V., Deng, G., Nakajima, K., Tabatabai, Z. L., Ishii, N. and Dahiya, R. (2015). Long noncoding RNA MALAT1 promotes aggressive renal cell carcinoma through Ezh2 and interacts with miR-205. *Cancer Res.* **75**, 1322-1331. doi:10.1158/0008-5472.CAN-14-2931

Ji, P., Diederichs, S., Wang, W., Böing, S., Metzger, R., Schneider, P. M., Tidow, N., Brandt, B., Buerger, H., Bulk, E. et al. (2003). MALAT-1, a novel noncoding RNA, and thymosin beta4 predict metastasis and survival in early-stage non-small cell lung cancer. *Oncogene* **22**, 8031-8041. doi:10.1038/sj.onc.1206928

Li, Y., Luo, S., Dong, W., Song, X., Zhou, H., Zhao, L. and Jia, L. (2016). Alpha-2, 3-sialyltransferases regulate the multidrug resistance of chronic myeloid leukemia through miR-4701-5p targeting ST3GAL1. *Lab. Invest.* **96**, 731-740. doi:10.1038/labinvest.2016.50

Liu, Y.-C., Yen, H.-Y., Chen, C.-Y., Chen, C.-H., Cheng, P.-F., Juan, Y.-H., Chen, C.-H., Khoo, K.-H., Yu, C.-J., Yang, P.-C. et al. (2011). Sialylation and fucosylation of epidermal growth factor receptor suppress its dimerization and activation in lung cancer cells. *Proc. Natl. Acad. Sci. USA* **108**, 11332-11337. doi:10.1073/pnas.1107385108

Lopez-Beltran, A., Scarpelli, M., Montironi, R. and Kirkali, Z. (2006). 2004 WHO classification of the renal tumors of the adults. *Eur. Urol.* **49**, 798-805. doi:10.1016/j.eururo.2005.11.035

Mendelsohn, J. and Baselga, J. (2006). Epidermal growth factor receptor targeting in cancer. *Semin. Oncol.* **33**, 369-385. doi:10.1053/j.seminoncol.2006.04.003

Miyagi, T. (2008). Aberrant expression of sialidase and cancer progression. *Proc. Jpn. Acad. Ser. B Phys. Biol. Sci.* **84**, 407-418. doi:10.2183/pjab.84.407

Motzer, R. J., Bacik, J. and Mazumdar, M. (2004). Prognostic factors for survival of patients with stage IV renal cell carcinoma: memorial sloan-kettering cancer center experience. *Clin. Cancer Res.* **10**, 6302S-6303S. doi:10.1158/1078-0432.CCR-040031

Pilatte, Y., Bignon, J. and Lambré, C. R. (1993). Sialic acids as important molecules in the regulation of the immune system: pathophysiological implications of sialidases in immunity. *Glycobiology* **3**, 201-218. doi:10.1093/glycob/3.3.201

Ponting, C. P., Oliver, P. L. and Reik, W. (2009). Evolution and functions of long noncoding RNAs. *Cell* **136**, 629-641. doi:10.1016/j.cell.2009.02.006

Qin, R., Chen, Z., Ding, Y., Hao, J., Hu, J. and Guo, F. (2013). Long non-coding RNA MEG3 inhibits the proliferation of cervical carcinoma cells through the induction of cell cycle arrest and apoptosis. *Neoplasma* **60**, 486-492. doi:10.4149/neo_2013_063

Raveh, E., Matouk, I. J., Gilon, M. and Hochberg, A. (2015). The H19 Long non-coding RNA in cancer initiation, progression and metastasis - a proposed unifying theory. *Mol. Cancer* **14**, 184. doi:10.1186/s12943-015-0458-2

Rini, B. I. (2006). Stabilization of disease in patients with metastatic renal cell carcinoma using sorafenib. *Nat. Clin. Pract. Oncol.* **3**, 602-603. doi:10.1038/ncponc0634

Schlessinger, J. (2014). Receptor tyrosine kinases: legacy of the first two decades. *Cold Spring Harb. Perspect Biol.* **6**, a008912. doi:10.1101/cshperspect.a008912

Seles, M., Hutterer, G. C., Kiesslich, T., Pummer, K., Berindan-Neagoe, I., Perakis, S., Schwarzenbacher, D., Stotz, M., Gerger, A. and Pichler, M. (2016). Current insights into long non-coding RNAs in renal cell carcinoma. *Int. J. Mol. Sci.* **17**, 573. doi:10.3390/ijms17040573

Shaulian, E. and Karin, M. (2002). AP-1 as a regulator of cell life and death. *Nat. Cell Biol.* **4**, E131-E136. doi:10.1038/ncb0502-e131

Stumm, G., Eberwein, S., Rostock-Wolf, S., Stein, H., Pomer, S., Schlegel, J. and Waldherr, R. (1996). Concomitant overexpression of the EGFR and erbB-2 genes in renal cell carcinoma (RCC) is correlated with dedifferentiation and metastasis. *Int. J. Cancer* **69**, 17-22. doi:10.1002/(SICI)1097-0215(19960220)69:1<17::AID-IJC4>3.0.CO;2-Z

Veale, D., Kerr, N., Gibson, G. J., Kelly, P. J. and Harris, A. L. (1993). The relationship of quantitative epidermal growth factor receptor expression in non-small cell lung cancer to long term survival. *Br. J. Cancer* **68**, 162-165. doi:10.1038/bjc.1993.306

Wang, L., Cai, Y., Zhao, X., Jia, X., Zhang, J., Liu, J., Zhen, H., Wang, T., Tang, X., Liu, Y. et al. (2015a). Down-regulated long non-coding RNA H19 inhibits carcinogenesis of renal cell carcinoma. *Neoplasma* **62**, 412-418. doi:10.4149/neo_2015_049

Wang, M., Huang, T., Luo, G., Huang, C., Xiao, X.-Y., Wang, L., Jiang, G.-S. and Zeng, F.-Q. (2015b). Long non-coding RNA MEG3 induces renal cell carcinoma cells apoptosis by activating the mitochondrial pathway. *J. Huazhong Univ. Sci. Technolog. Med. Sci.* **35**, 541-545. doi:10.1007/s11596-015-1467-5

Warren, L., Fuhrer, J. P. and Buck, C. A. (1972). Surface glycoproteins of normal and transformed cells: a difference determined by sialic acid and a growth-dependent sialyl transferase. *Proc. Natl. Acad. Sci. USA* **69**, 1838-1842. doi:10.1073/pnas.69.7.1838

Wee, P. and Wang, Z. (2017). Epidermal growth factor receptor cell proliferation signaling pathways. *Cancers (Basel)* **9**, 52. doi:10.3390/cancers9050052

Wen, K.-C., Sung, P.-L., Hsieh, S.-L., Chou, Y.-T., Kuang-Sheng Lee, O., Wu, C.-W. and Wang, P.-H. (2017). alpha2,3-sialyltransferase type I regulates migration and peritoneal dissemination of ovarian cancer cells. *Oncotarget* **8**, 29013-29027. doi:10.18632/oncotarget.15994

Wu, Y., Liu, J., Zheng, Y., You, L., Kuang, D. and Liu, T. (2014). Suppressed expression of long non-coding RNA HOTAIR inhibits proliferation and tumourigenicity of renal carcinoma cells. *Tumour Biol.* **35**, 11887-11894. doi:10.1007/s13277-014-2453-4

Yen, H.-Y., Liu, Y.-C., Chen, N.-Y., Tsai, C.-F., Wang, Y.-T., Chen, Y.-J., Hsu, T.-L., Yang, P.-C. and Wong, C.-H. (2015). Effect of sialylation on EGFR phosphorylation and resistance to tyrosine kinase inhibition. *Proc. Natl. Acad. Sci. USA* **112**, 6955-6960. doi:10.1073/pnas.1507329112

Zhou, C., Huang, C., Wang, J., Huang, H., Li, J., Xie, Q., Liu, Y., Zhu, J., Li, Y., Zhang, D. et al. (2017). LncRNA MEG3 downregulation mediated by DNMT3b contributes to nickel malignant transformation of human bronchial epithelial cells via modulating PHLPP1 transcription and HIF-1alpha translation. *Oncogene* **36**, 3878-3889. doi:10.1038/onc.2017.14